Article

Crude Oil Drop Penetration into Permeates Using a Slotted Pore Membrane

Asmat Ullah,* Saad Ullah Khan, Kamran Alam, Umar Wahid, and Victor Mikhilovich Starov

Read Online

ACCESS | Metrics & More | Article Recommendations

ABSTRACT: The primary focus of the presented research is to come up with a model that could be utilized to evaluate the permeate content (concentration) of oil drops using a straight (nonconverging) slotted microstructured membrane. The content (concentration) of crude drops in the permeate with a non-converging slit structure membrane has not been studied before, and the study presented would be a good contribution to the literature. A comparison between the use of a converging (narrowing toward the inside) and a nonconverging slotted pore microstructured membrane is made for the purpose of removing oil content from the produced water. Due to the drag force, the droplets pass through the membrane slots; however, the static force acts in the opposite direction and tries to reject droplets by the membrane. At a certain point, these two forces balance the effect of each other, which is known as "100% cutoff through the membrane". A linear line is obtained by joining the 100% cutoff or rejection point to the 0% rejection point, which is referred to as the "linear fit" in this paper. The linear fit approach could be utilized for estimating rejection below the 100% cutoff point. Various types of crude oil drops obtained from different locations were analyzed experimentally, and the results were compared with the presented model. The proposed model was found to be in agreement with the different types of oil drops. Experimental and predicted results showed that the nonconverging slotted microstructured membrane provided low friction to oil drops through the membrane as compared to the converging slots. Furthermore, the developed model can be utilized to predict the overall oil content in the permeate. This research has great importance and will allow researchers around the globe to estimate crude oil concentration within the allowable limits.
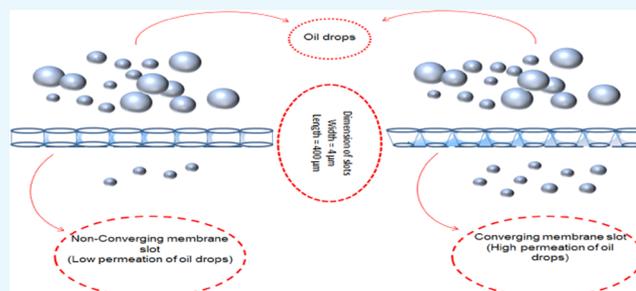
1. INTRODUCTION

In the 19th century, the industrial revolution led to enhanced energy demands, and as a result, oil, gas, and coal exploration increased drastically. The huge exploration of oil and gas resulted in the generation of many waste byproducts, including produced water, which is among the largest waste liquids containing organic and inorganic chemicals, heavy metals, as well as dissolved oil. Due to the hazardous nature of the produced water, it possess a huge threat to human beings as well as aquatic animals.[1,2] Dissolved and crude oil drops in the form of emulsions in produced water play a significant role, and the friction of crude oil in produced water depends on the location of the well as well as on the age of the reservoir. Crude oil presence in produced water is a serious environmental problem causing severe damage to both aquatic and human lives. Therefore, to address this problem, the direct disposal of waste streams of produced water in the environment is strictly prohibited and is monitored according to international stand-ards.[3−5] According to international standards, on monthly and daily bases, the allowable limits for oil in waste streams are 29 and 42 mg L^{-1}, respectively.[6,7] Similarly, for Northeast Atlantic oil and gas production plants, the allowable limit for oils in

produced water is up to 30 mg L^{-1} before disposing the oil into natural water resources.[7,8] To meet the above requirements, the produced water should be effectively treated before its disposal into seawater.

Conventional oil−water emulsion separation techniques such as flotation,[9] gravitational settling tanks,[10] and adsorption[11] were not found to be effective for separation of oil droplets below 20 μm.[12] To address this issue, porous structured membranes were investigated for effective oily water treatment, which play a prominent role in oil/water (O/W) separation; in addition, they have several advantages such as no addition of chemicals, continuous operation, high rejection of oil drops, and high permeation.[13]

A wide range of microfiltration (MF)[14−20] and ultrafiltration (UF)[21−26] methods for O/W separation have been evaluated. The published literature showed that MF and UF filtration processes were analyzed on the basis of the permeate flux rate and the transmembrane pressure (TMP) for O/W separation. The UF process takes place at TMP and gives a low permeate flux rate, which seem to be economically unattractive for offshore platforms,[27−29] while the MF process occurs at low transmembrane pressures and gives a high permeate flux rate, which make the process more significant for the commercial application of oil−water separation.[29]

The MF separation technique uses two different modes: surface filtration (particulates retained on the surface of the membrane) and depth filtration (particulates retained inside the pores of the membrane).[30] In depth filtration, particles retained inside the membrane pores and cleaning is difficult.[31] On the other hand, in surface filtration the particles retained on the membrane surface and cleaning is relatively easier.[17] In addition to the MF mode, different membrane pore structures were studied by different researchers,[32−35] and it was observed that membrane pore structures play a significant role in separation as well in membrane fouling. Initially, the circular pore membrane was thoroughly studied, and the results showed that a small circular pore membrane produced a high transmembrane pressure compared to bigger circular pore membranes.[17] However, current studies demonstrated that slotted pore membranes have better performance as compared to circular pore membranes in terms of oil−water separation and permeate flux rates.[18,29,36−40] Drops pass through a circular pore membrane due to transmembrane pressure (TMP); on the other hand, the drag force created by the flow of fluid around drops allows passage of drops in the case of a slotted pore membrane.[36−39] Moreover, a complete blocking occurs in the case of a circular pore membrane, while a slotted pore membrane faces partial blocking.[38]

Recent modeling studies focus on the action of an individual oil droplet through the slotted pore membrane; mathematical relations have been established for the two key scenarios of oil droplets (permeation and rejection) and have been shown to be dependent on the droplet size, shear rate, surface tension, viscosity of the fluid, and the size of the membrane slots.[20,29] Furthermore, on the basis of these mathematical relations, the permeate oil concentration has been predicted for the converging membrane slots and validated with experimental data points.[39] There has been no theoretical study conducted for the prediction of oil drops in permeates through a nonconverging membrane slot.

Lastly, the permeate concentration of oil drops in produced water is an important factor, and it should be below the concentration of oil drops in the produced water set by international bodies for discharging it into the sea. The main objective of the presented research work is to come up (develop) with an analytical model that can predict the permeate concentration of oil drops through a nonconverging slotted pore membrane. The presented model is based on the calculation of 100% rejection points or 100% cutoff points from the balance of two forces (static and drag) acting on oil drops while passing through the membrane. The 100% rejection points were extended to the origin of rejection graphs, and permeated oil drops were calculated by the multiplication of the portion of permeated drops with oil drops in the permeate. Furthermore, the permeate concentrations of converging and nonconverging slotted pore membranes were also compared

under the same operating conditions; the role of slot shape on the rejection and permeation of oil drops through the membrane was also thoroughly investigated. Three different types of oil drops were studied for the generalization of the theoretical study. A novel approach was considered for the prediction of permeate concentration and the influence of membrane slot type on the rejection and permeation of oil drops through the membrane.

Oil in water is a huge potential threat for living organisms within the waters and is also harmful to the environment. Crude oil contents in produced water that are rejected into oil and gas wells or discharged into the sea should be 10 and 30 ppm, respectively. Crude oil concentration above the permissible limits in permeates could be a huge threat to the environment in both onshore and offshore. Therefore, evaluation of crude oil concentration in permeates is of great importance for researchers around the world. Further, slotted pore membranes provide a unique structure that allows high permeate flux to pass through them by the drag force and do not permit foulents to pass into the permeate. Slotted pore membranes could be the new area for researchers to explore, specially regarding oil−water separation at both the lab and industrial scales.

2. THEORY

Mathematical approaches have been investigated for the penetration of deformable oil spherical drops for the estimation of static force in the cases of both nonconverging (straight) and converging (narrowing toward the inside) slotted pore membranes and are provided in eqs 1 and 2, respectively.[20,29]

$$F_{cx} = 2\pi\sigma\left(\frac{3R_{sp}^2}{h} + \frac{h^2}{1 - \frac{h^3}{R_{sp}^3}}\frac{1}{R_{sp}}\left(\frac{3}{2} - \tanh^{-1}\sqrt{1 - \frac{h^3}{R_{sp}^3}}\right.\right.$$
$$\left.\left.\times\frac{3h^3}{2R_{Sp}^3\sqrt{1 - \frac{h^3}{R_{sp}^3}}}\right) - 4R_{sp}\right)$$

$$F_{cx}* = -\left(2\pi R_{sp}\sigma\left(\left(\frac{sh}{R_{sp}} + \left(-3\left(\frac{h}{R_{sp}}\right)^3\right.\right.\right.\right.$$
$$- \arccos\left(\frac{h}{R_{sp}}\right)^3\frac{1}{\sqrt[2]{1 - \left(\frac{h}{R_{sp}}\right)^6}}\left(-8\left(\frac{h}{R_{sp}}\right)^6\right)$$
$$\left.\left.\left.\left.+ 2\middle/\left(\frac{h}{R_{sp}}\sqrt{1 - \left(\frac{h}{R_{sp}}\right)^6}\right)^2\right)\right)\right)\times \sin\frac{\alpha}{2}\right) \tag{2}$$

Equations 1 and 2 state that the static force is a function of the interfacial tension between O/W, size of oil drops, and width of the slot of the membrane. Equation 2 also illustrates that the static force also depends on the angle of depletion of the slot for the converging slot. A mathematical model has been presented

by[41] for the drag force of oil drops (eq 3), which is dependent on fluid viscosity, velocity, and oil drop size. It can be seen in Figure
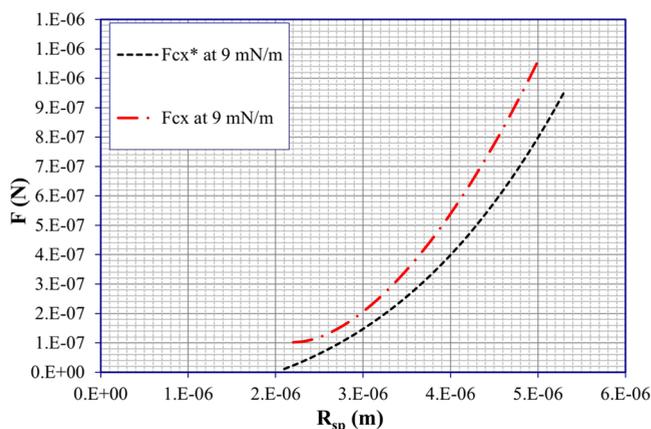

Figure 1. Comparison of static forces for nonconverging slots (Fcx) using eq 1 and converging slots (Fcx*) using eq 2 at 9 mN m^{-1} interfacial tension between oil and water phases.

1 that a higher static force is noticed when using nonconverging slots as compared to converging slots.

$$\mathbf{F_d} = \mathbf{k_w} 12\pi\mu\mathbf{R_{sp}}\mathbf{U} \tag{3}$$

When oil drops pass through membrane slots, two types of forces come into play: static force and drag force. Static forces act in the upward direction and try to reject oil drops from the membrane. Similarly, drag forces push the drops in the downward direction and help oil drops pass through the membrane. The balance of these two forces on oil drops is termed as 100% rejection points or 100% cutoff points.[29] It is the point that decides which drops will penetrate (pass) through the pore of the membrane and which drops will be retained by the membrane. In more simple words, drops below the 100% cutoff points can pass through the membrane and drops higher than the 100% cutoff points cannot pass and will be rejected by the membrane. The rejection points depend on the static and drag forces of oil drops, meaning that different rejection points are expected at different interfacial tensions of oil drops and at different flux rates of oil drops.

The 100% rejection points are calculated for different types of oil drops at a different flux rate and have been extended to the origin of rejection graphs to calculate the portion of permeated oil drops. The permeate concentration of oil drops was calculated by multiplication of the permeated portion of oil drops from the rejection graph with oil drops in the feed.

At 100% rejection or cutoff point where the drag and static forces are in equilibrium mainly depends on the interfacial tension between continuous and dispersed phases in cases of both converging (narrowing toward the inside) and straight (nonconverging) slots. At higher interfacial tension, the static force equalizes the drag force at a smaller drop size as compared to the lower interfacial tension for the nonconverging and converging slots. Oil drops stabilized with PVA and Tween 20 providing interfacial tensions of 4 and 9 mN m^{-1}, respectively, were tested experimentally and using the model. At a higher interfacial tension, the drag force was balanced by the static force at a smaller drop size in cases of both converging and nonconverging slots. At higher interfacial tension, the drops were more rigid and had a higher tendency to restore their

spherical shape when they were forced to deform and pass through the slots of the membrane. Oil drops with interfacial tensions of 4 and 9 mN m^{-1} were subjected to various in-pore filtration velocities of 0.04, 0.08, and 0.12 m s^{-1}. The 100% cutoff or 100% rejection point (where Fcx and Fd intersect) considerably changed with a change in filtration velocities, as can be seen in Figure 2a,b. If the highest filtration velocity (0.12 m
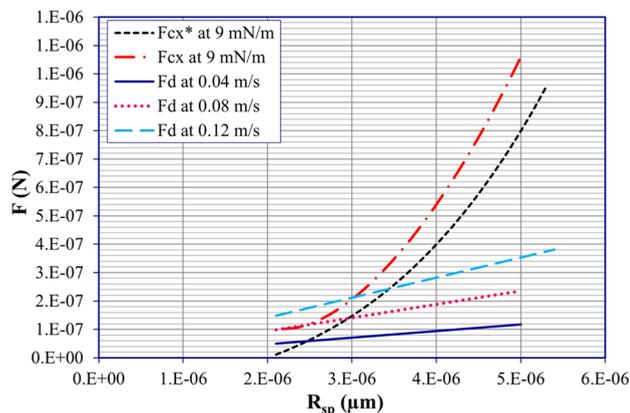
a
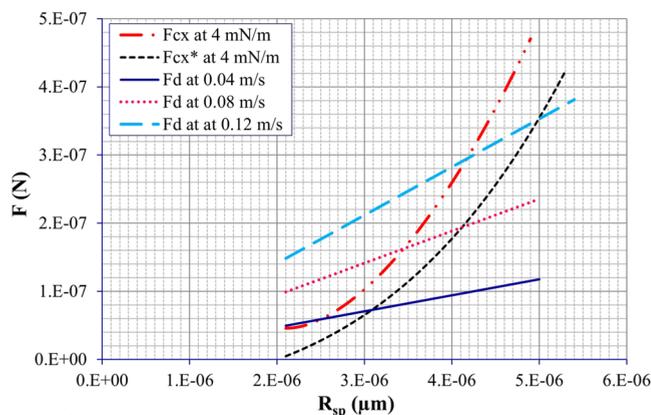
b

Figure 2. (a) Drag and static forces against drop radius at various filtration velocities and an interfacial tension of 9 mN m^{-1}. (b) Drag and static forces against drop radius at various filtration velocities and an interfacial tension of 4 mN m^{-1}.

s^{-1}) inside the slot is considered in Figure 2a, the drag force equalizes by the static force at a drop size of 6 μm in the case of the nonconverging slot, while the same situation occurs at 7.4 μm drop size under the same conditions. It implies that a converging slot allows a higher portion of oil drops to be passed as compared to the nonconverging slots when subjected to the same conditions. Similarly, at interfacial tension 4 μm and the highest in-slot filtration velocity of 0.12 m s^{-1}, the drag force is equalized by the static force at drop sizes of 8.4 and 10 μm in cases of using nonconverging and converging slots, respectively, as can be seen in Figure 2b. This shows that interfacial tension also plays a vital role in the penetration (passage) of drops through the membrane slots.

3. MATERIAL AND METHODS

3.1. Materials. Crude oil (22, 27, and 30 °API) having content (concentration) of oil in water 400 ppm, supplied by North sea oil companies, was used in the present research work.

Oil drops produced in Tween 20 (polyoxyethylene sorbitan monolaurate) dissolved in water was also utilized in the research study, which was provided by Fluka, U.K. Deionized water was used for the continuous phase, and oil was used as the dispersed phase for the O/W emulsion preparation. A magnetic stirrer (model: SM1 Stuart Scientific U.K.) was used to produce the desired drop in the size range of $1-15~\mu$m by varying the speed and time. A Du-Nouy Ring apparatus was used for the measurement of interfacial tension of oil drops. To find the number of scattered droplets and their concentration, a Coulter Multisizer II (model: Coulter Counter, Coulter Electronics Ltd.) was used. Equation 4 was used to measure the concentration of oil droplets entered and recovered by Coulter.

$m = \pi/6$ (no. of droplets) (mid-size of droplet dia)^3 (density of droplets)

$$m = \frac{\pi}{6}(p_f) \sum k_i x_i^3 \tag{4}$$

The model of the linear fit approach was validated by the genuine data of produced water obtained from ref 42.

3.2. Filtration. A slotted pore membrane was used for filtration experiments adopting the dead-end candle micro-filtration configuration as shown in Figure 3. The dimension of
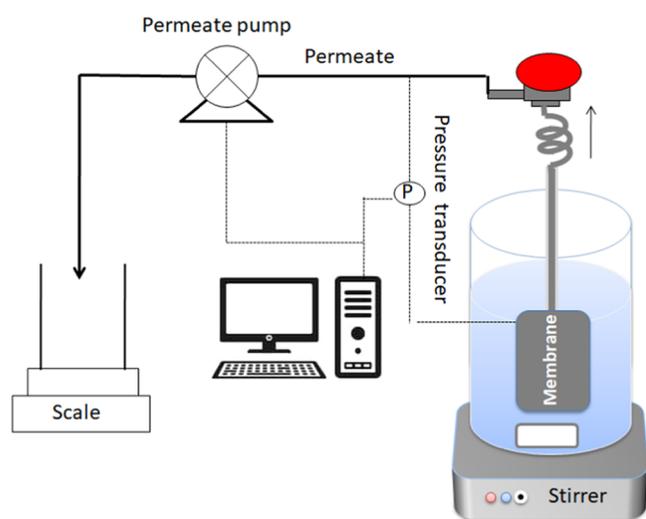

Figure 3. Experimental setup for the dead-end candle microfiltration system.

the slot used was width 4 μm, length 400 μm, and thickness of the membrane 300 μm, supplied by Micro-pore Technologies Limited, U.K. The density of the slot was 9.2×10^6 slot m^{-2} with the surface porosity being 1.4%.

Modification in the surface of the membrane was made with poly(tetrafluoroethylene) (PTFE). It was immersed in a feed beaker, and a peristaltic pump (having model no. RS 440−515, Neutral, U.K.; a type of electric operated positive displacement pump that can maintain constant flux conditions) was used to control the permeate suction. A measuring cylinder was used for the collection of permeate and was periodically returned to the feed container. A pressure transducer by Farnell, U.K., having model no. HCX001A60 was used to measure pressure across the membrane, which has a resolution of 0.1 psi. The experimental setup is shown in Figure 3 below.

The deformation of oil droplets can be observed from the existence of big-size oil droplets in the permeate through membrane slots. The surface of the slotted membrane was

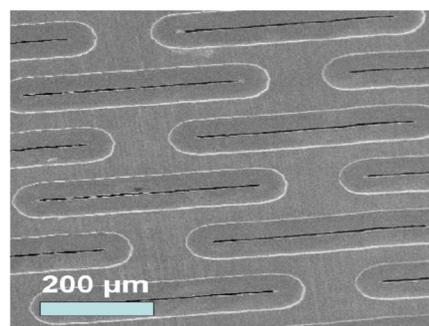studied through scanning electron microscopy (SEM), as displayed in Figure 4.

Figure 4. Scanning electron microscope image of the surface of the slotted pore structured membrane.

Equation 5[43] was used for the calculation of the grade efficiency.

$$\text{grade efficiency} = \left(1 - \frac{\text{permeate mass concentration in size grade}}{\text{feed mass concentration in size grade}}\right) \times 100 \tag{5}$$

The effect of flux rate on grade efficiency and 100% cutoff points was measured by varying the flow rate of the permeate through the membrane. The membrane was washed with 2% Ultrasil 11 and hot filtered water (50 °C) before and after each run. Various permeate flux rates were obtained at different transmembrane pressures with the assumption of the membrane being clean and ready for reuse until the change in flux per unit time became similar to that of clean water.

4. RESULTS AND DISCUSSION

Figure 5a presents the concentration of crude oil drops in the feed.[39] When oil drops pass through the membrane slot, static force and drag force come into play. As discussed earlier, the static force is accountable for the retention (rejection) of the drops from the membrane, and it was calculated from eq 1 using a nonconverging (straight) slotted pore membrane.[29] Also, there is a linear relationship between the drag force and interfacial tension of oil drops between the dispersed and continuous phases.[29] Drag force on the other side helps the drops pass through the membrane, and it was calculated from eq 3. A point of 100% cutoff points or 100% rejection points is reached when it is very hard for the drag force to deform the drop further and to pass it through the slotted pore membrane. The linear fit approach was used for the calculation of permeated drops below the 100% cutoff points. It was obtained from a linear line by extrapolating 100% cutoff points to the origin of rejection graphs. The portion of permeated oil drops was calculated from the linear fit approach and was multiplied by the concentration of crude oil drops in the feed to predict the permeate concentration. Different permeate concentrations were obtained at a different flux rate and at a different interfacial tension. The predicted permeate concentrations (of 22, 27, and 30 °API) are presented in Figure 5b−d. The concentrations (in ppm) of 22 and 27 °API oil drops in the permeate are presented in Table 2 for different flux rates, while the concentration (in ppm) of 30 °API crude oil drops in the permeate is illustrated in
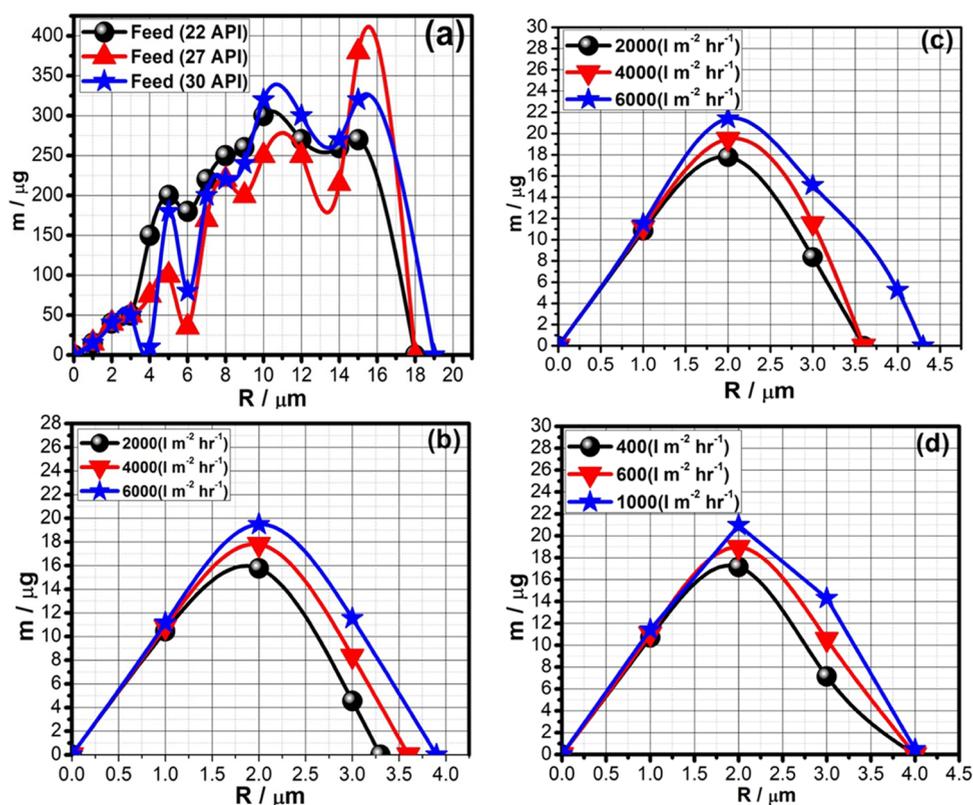
Figure 5. (a) Concentrations of 22, 27, and 30 °API crude oil drops in the feed, while (b−d) show permeate concentrations of crude oil drops using a nonconverging membrane slot calculated from the 100% cutoff points.

Table 3. It can be observed from Tables 2 and 3 that on increasing the flux rate, the concentration of crude oil increases; it is because the increasing flux rates increase the velocity of the oil fluid, which increases the drag force on the oil drops and helps more numbers of oil drops pass through the slot of the membrane. Moreover, Tables 2 and 3 further illustrate that on increasing the °API value of the drops, the concentration of crude oil drops in the permeate decreases because the interfacial tension of oil drops increases, as a result of which the static force increases (eq 1). It shows that the permeation of oil drops through the slotted pore membrane is strongly dependent on the flux rate and the interfacial tension of oil drops, which affects the drag and static forces, respectively. These results are in agreement with the published results of.[29,39]

The permeate concentrations of crude oil drops 22 °API, 27 °API, and 30 °API for the converging slotted pore membrane are presented here from the work of,[39] and the same is compared with the permeate concentration of the nonconverging slotted pore membrane under the same operating condition. Figure 6a−c shows the comparison of converging and nonconverging membrane slots for 22 °API crude oil drops in the permeate, Figure 6d−f shows the comparison for 27 °API crude oil drops in the permeate, while Figure 7a−c shows the comparison for 30 °API crude oil drops in the permeate. It can be easily observed from Figures 5 and 6 that the concentration of crude oil drops in the permeate is higher for the converging membrane slots compared to the nonconverging membrane slots. In addition, a larger number of crude oil drops passes through the converging membrane slot than through the nonconverging membrane slots. The concentrations (in ppm) of crude oil drops 22, 27, and 30 °API through the converging and nonconverging membrane slots are presented in Tables 1 and 2. Under the same operating

conditions, the converging membrane slots give a higher permeate concentration of crude oil (average of 35.5% for 22 °API, 17% for 27 °API, and 38.6% for 30 °API crude oil drops) than the permeate concentration of nonconverging membrane slots, indicating that oil drops show a high static force for the nonconverging slotted microstructured membrane as compared to the static force for the converging slotted pore membrane. Similar results were also reported by[39] that sudden deformation of oil drops occurs through the converging slotted pore membrane, which leads to low static force and high permeation of oil drops through the membrane, while gradual deformation of oil drops occurs, which leads to a higher static force and a low number of drops passes through the membrane under the same operating conditions including the flux rate, interfacial tension, size, and length of the membrane slot.

Similarly, Tween 20 oil drops dissolved in water were studied to elaborate the effect of the nature of different oil drops by adopting the same approach as above. First, 100% rejection points were calculated for oil drops in Tween 20 dissolved in water, and then, a linear fit approach was used to calculate the permeate concentration. The concentrations of oil drops in the feed and permeate at different in-pore filtration velocities are presented in Figure 8. Figure 8a shows the % mass concentration of oil drops (g g^{-1}) through the nonconverging slotted pore membrane, while Figure 8b represents the % mass concentration of oil drops (g g^{-1}) through the converging slotted pore membrane. It can be observed from Figure 7b that a higher number of drops passes through the converging slotted pore membrane compared to the nonconverging slotted pore membrane (Figure 8a). Almost all oil drops are rejected by the nonconverging slotted pore membrane at 0.04 m s^{-1} in-pore filtration velocity, as shown in Figure 8a, while for the
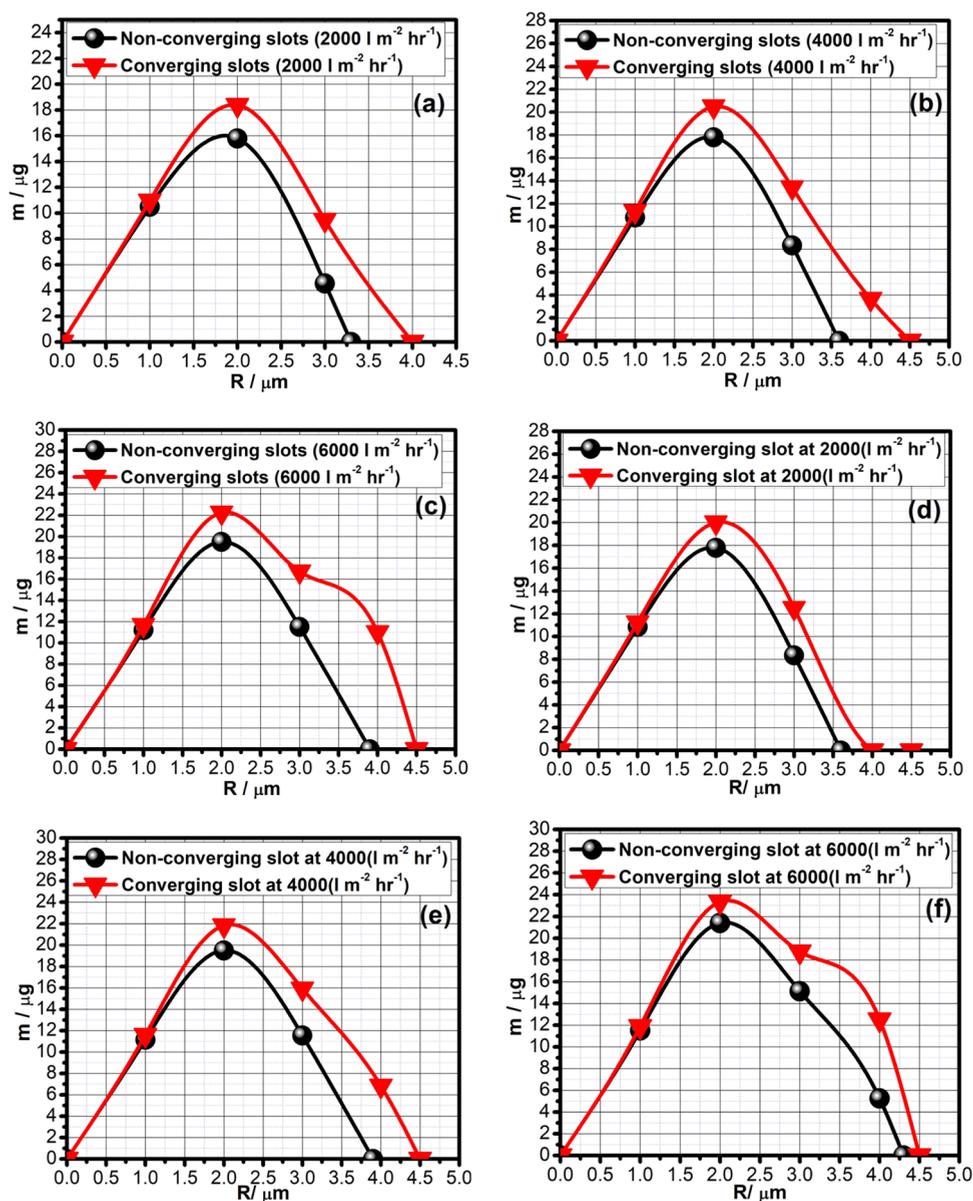
Figure 6. Permeate oil contents (concentrations) through converging (narrowing toward the inside) and nonconverging membrane (straight) slots at different flux rates. (a−c) shows the 22 °API crude oil drops, and (d−f) shows the 27 °API crude oil drops.

converging slotted pore membrane, still a large number of drops pass through the membrane at the same velocity (0.04 m s^{-1}), (Figure 8b). As the in-pore filtration velocity increases, the number of oil drop permeation increases, which has been observed for both types of membrane slots; however, when these two slots are compared on the basis of the same in-pore filtration velocity, a large number of drops passes through the converging slotted pore membrane. It has been noted that the same results were observed in the previous model based on the feed of North oil sea companies and with the result reported by[29] for deforming oil drops while passing through the converging and nonconverging slotted pore membranes.

To validate these models, crude oil drops in real produced water samples were studied. Genuine data of crude oil drops from different oil fields with different interfacial tensions (°API value) are plotted in Figure 9a,b, as have been reported elsewhere.[42] These data were obtained from different locations that are operating oil fields in Kuwait. The data were used to

demonstrate and validate the approach used for the estimation of the concentration of crude oil drops in the permeate. Figure 9c shows the predicted permeate concentration of 29 °API crude oil drops of Bair Aquifer water, while Figure 9d shows the predicted permeate size distribution of 29 °API crude oil drops of oil effluent water. Similarly, Figure 8e shows the predicted permeate size concentration of 32 °API crude oil drops in Bair Aquifer water, while Figure 8f shows the predicted permeate concentration of 32 °API crude oil drops in oil effluent water. The predicted permeate concentrations (in ppm) of these crude oil drops with different interfacial tensions and different flux rates have been presented in Table 3. Concentrations of crude oil drops (29 °API) in the feed of oil field effluent water and Bair Aquifer water were 1.5 and 1 ppm, respectively, as reported.[42] Similarly, the concentrations of crude oil drops (32 °API) in the feed of oil field effluent water and Bair Aquifer water were 26 and 17 ppm, respectively, the same as have been reported in ref 42. Predicted permeate concentrations of these oil drops are shown
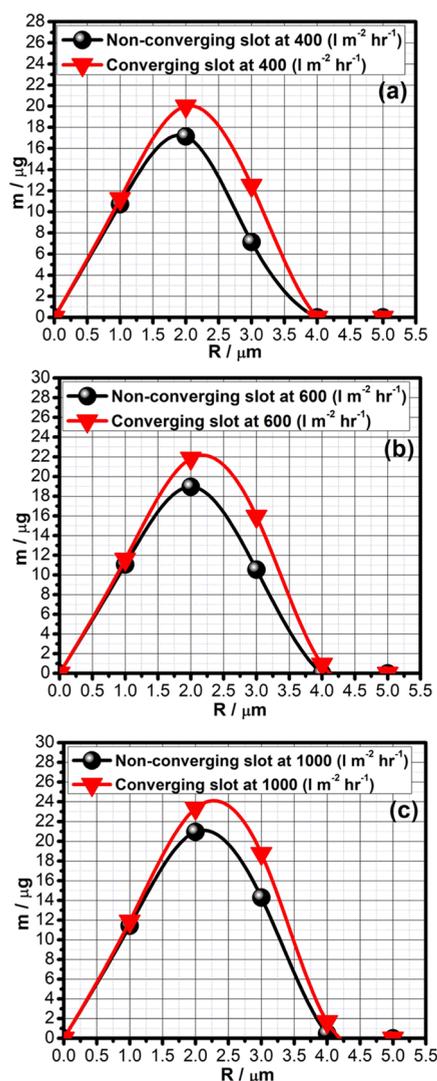
Figure 7. (a−c) Permeate concentration of 30 °API crude oil drops using converging (narrowing toward the inside) and nonconverging (straight) membrane slots at different flux rates.

Table 2. Permeate Concentration (in ppm) of 30 °API Crude Oil Drops Using Converging (Narrowing toward the Inside) and Nonconverging (Straight) Slotted Pore Membranes at Various Flux Rates

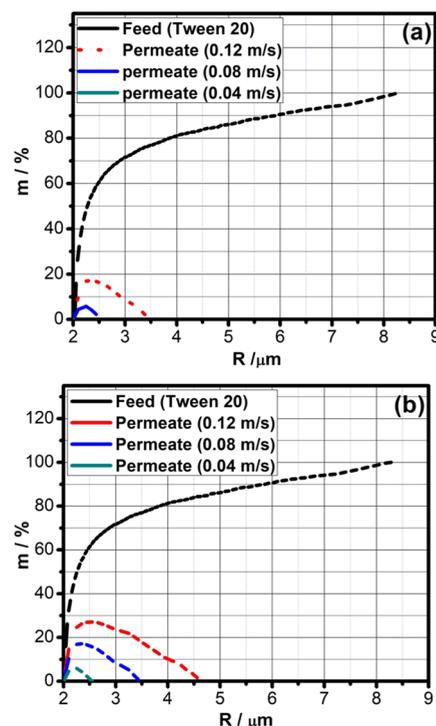| flux rate (L m^{-2} h^{-1})	crude oil drops (30 °API) through converging slots (in ppm)	crude oil drops (30 °API) through nonconverging slots (in ppm)	% difference in permeation of concentration of crude oil drops
400	21	12.5	41
600	24	14.4	40
1000	26	16.8	35

Figure 8. Feed and permeate concentrations of oil drops (by mass %) in Tween 20 dissolved in water at different in-pore filtration velocities. (a) Nonconverging slotted-type pore membrane. (b) Converging slotted-type pore membrane.

in Table 3. Using the linear fit approach, the permeate concentration (29 and 32 °API) reduced significantly, less than 1 ppm for all samples of crude oil drops through the nonconverging slotted pore membrane. Similarly, Table 4 shows the permeate concentration of the same crude oil drops through the converging slotted pore membrane reported from ref 39. Comparing Tables 3 and 4, it is clear that there was a higher permeate concentration of crude oil drops for the converging membrane slots than for nonconverging membrane slots, which also shows the correspondence with the results of crude oil

drops (22 °API, 27 °API, 30 °API) that have been presented earlier in this discussion for the deforming oil.[29]

5. CONCLUSIONS

A new model has been developed for estimating the permeate concentration of oil drops through a straight (nonconverging) slotted microstructured membrane, which is based on the rejection and permeation of oil drops through the membrane, calculated from the 100% rejection point. Prediction of crude oil concentration in the permeate was evaluated before, and the idea

Table 1. Permeate Concentration (in ppm) of 22 and 27 °API Crude Oil Drops Using Converging (Narrowing toward the Inside) and Nonconverging (Straight) Membrane Slots at Different Flux Rates

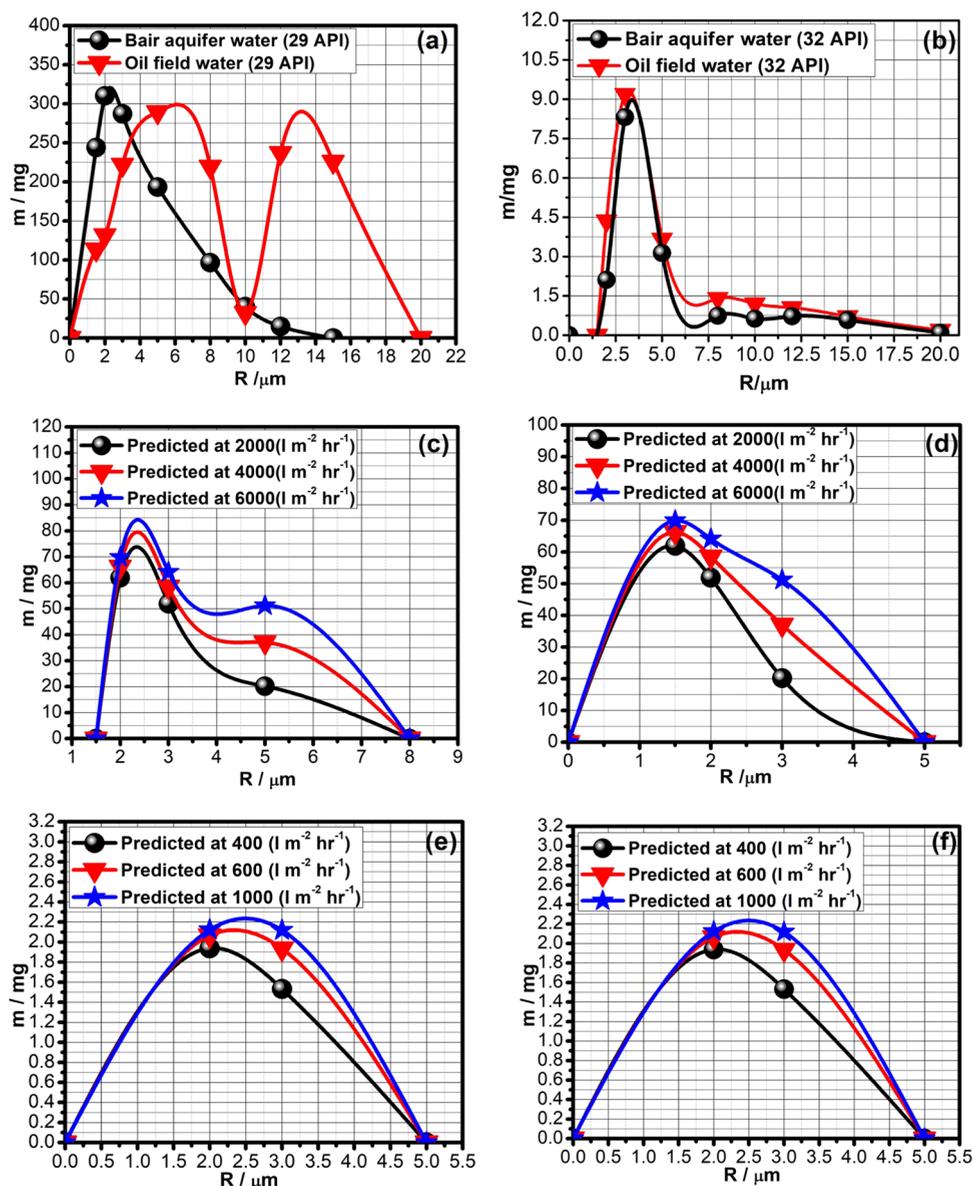| flux rate (L m^{-2} h^{-1})	crude oil drops (22 °API) through converging slots (in ppm)	crude oil drops (22 °API) through nonconverging slots (in ppm)	% difference in permeate concentration of crude oil drops (22 °API)	crude oil drops (27 °API) through converging slots (in ppm)	crude oil drops (27 °API) through nonconverging slots (in ppm)	% difference in permeate concentration of crude oil drops (27 °API)
2000	16	10	37	18	15	16
4000	19	12	36	22	17	22
6000	21	14	33	24	21	13

Figure 9. (a, b), Feed concentrations of 29 and 32 °API crude oil drops obtained from oil fields working in Kuwait. (c, d) Permeate concentration of 29 °API crude oil drops of Bair aquifer water and oil field water, respectively. (e, f) Permeate concentration of 32 °API cure oil drops of Bair aquifer and oil field water, respectively, using a nonconverging membrane slot.

Table 3. Permeate Concentrations of Crude Oil Drops (in ppm) of Oil Field Effluent Water and Bair Aquifer Water through the Nonconverging (Straight) Membrane Slot at Different Flux Rates

flux rate ($L\ m^{-2}\ h^{-1}$)	crude oil drops (29 °API) in oil field effluent water (ppm)	crude oil drops (29 °API) in Bair Aquifer water (ppm)	crude oil drops (32 °API) in Bair Aquifer water (ppm)	crude oil drops (32 °API) in produced water (ppm)
2000	0.13	0.28	0.230.28	3.5
4000	0.16	0.33	0.29	4
6000	0.19	0.37	0.29	4.24

Table 4. Permeate Concentrations of Crude Oil Drops (in ppm) of Oil Field Effluent Water and Bair Aquifer Water through the Converging (Narrowing toward the Inside) Membrane Slot at Different Flux Rates

flux rate ($L\ m^{-2}\ h^{-1}$)	crude oil drops (29 °API) in oil field effluent water (ppm)	crude oil drops (29 °API) in Bair Aquifer water (ppm)	crude oil drops (32 °API) in Bair Aquifer water (ppm)	crude oil drops (32 °API) in produced water (ppm)
2000	0.017	0.015	0.09	0.3
4000	0.022	0.02	0.13	0.36
6000	0.03	0.027	0.15	0.46

could be of great importance for researchers working in the field. The 100% rejection was calculated from the balance of the static and drag forces acting on oil drops during passing through the membrane, which was extended to the origin of the rejection graph, known as the linear fit approach. Using this approach, the

theoretical permeate concentration of oil drops was calculated obtained from various locations. Three different types of oil drops were used for the analysis of the study, and all types of oil drops show consistency with the results of the presented model. The model also shows dependency on the interfacial tension and

flux rate of oil drops. Furthermore, the permeate concentration of oil drops for the nonconverging membrane slot was also compared with the permeate concentration of oil drops for the converging membrane slot under the same operating condition (i.e., feed size distribution data, interfacial tension between the dispersed and continuous phase, flux rate, as well as size, structure, and length of the slot pore membrane). In the case of 30 °API crude oil drops, 41, 40, and 35% higher concentrations in the permeate were estimated at 200, 400, and 600 L m^{-2} h^{-1}, respectively, using the converging slotted pore membrane as compared to the nonconverging slotted pore membrane. All types of oil drops show consistency with the study of the comparison of permeate concentration using converging and nonconverging membrane slots. Nonconverging membrane slots reject a larger number of oil drops than converging membrane slots, and it is due to the gradual deformation of oil drops that occurs in the straight (nonconverging) slotted pore membrane, leading to a high static force, while sudden deformation of drops occurs in the converging slotted pore membrane, leading to a less static force, under the same operating condition. Furthermore, it will be more interesting if the results presented here obtained from the linear fit approach are validated with experimental data points after performing experiments. The study conducted here would be useful to find out whether the oil concentration in permeates is within the allowable limit set by international regularization bodies for discharge and should be the focus for researchers working in this area.

AUTHOR INFORMATION

Corresponding Author

Asmat Ullah − *Department of Chemical Engineering, University of Engineering & Technology Peshawar, Peshawar 25120 KPK, Pakistan;* ⓞ orcid.org/0000-0001-6278-3942; Email: a.ullah@uetpeshawar.edu.pk

Authors

Saad Ullah Khan − *Faculty of Materials and Chemical Engineering, GIK Institute of Engineering Sciences and Technology, Topi Swabi 23640, Pakistan*

Kamran Alam − *Faculty of Materials and Chemical Engineering, GIK Institute of Engineering Sciences and Technology, Topi Swabi 23640, Pakistan*

Umar Wahid − *Department of Chemical Engineering, University of Engineering & Technology Peshawar, Peshawar 25120 KPK, Pakistan*

Victor Mikhilovich Starov − *Department of Chemical Engineering, Loughborough University, Loughborough LE11 3TU, U.K.;* ⓞ orcid.org/0000-0003-0814-8870

Complete contact information is available at:
https://pubs.acs.org/10.1021/acsomega.1c03227

Notes

The authors declare no competing financial interest.

NOMENCLATURE

F_c static force (N)
F_d drag force (N)
h half of the width of the slot (m)
k_w correction factor for drag force
k_i number of droplets
R_{sp} radius of the spherical drop (m)
R_{ell} radius of the ellipsoid (spheroid) (m)
S_{ell} ellipsoid surface area (m^2)
S_{sp} sphere surface area (m^2)
U velocity inside the pore (m s^{-1})
X_i mid-size of the oil droplet (m)

Greek Symbols

σ interfacial tension (Nm^{-1})
α angle at which the slot converges toward the inside (deg)

μ Micron

ρ_f density of fluid (kg m^{-3})
η viscosity of fluid (Pa·s)

REFERENCES

(1) Utvik, T. I. R. Chemical characterisation of produced water from four offshore oil production platforms in the North Sea. *Chemosphere.* **1999**, *39*, 2593−2606.

(2) McCormack, P.; Jones, P.; Hetheridge, M. J.; Rowland, S. J. Analysis of oilfield produced waters and production chemicals by electrospray ionisation multi-stage mass spectrometry (ESI-MS^n). *Water Res.* **2001**, *35*, 3567−3578.

(3) Diya'uddeen, B. H.; Daud, W. M. A. W.; Aziz, A. R. A. Treatment Technologies for Petroleum Refinery Effluents: A Review. *Process Saf. Environ. Prot.* **2011**, *89*, 95−105.

(4) Farmaki, E.; Kaloudis, T.; Dimitrou, K.; Thanasoulias, N.; Kousouris, L.; Tzoumerkas, F. Validation of a FT-IR Method for the Determination of Oils and Grease in Water Using Tetrachloroethylene as the Extraction Solvent. *Desalination.* **2007**, *210*, 52−60.

(5) Mueller, S. A.; Kim, B. R.; Anderson, J. E.; Gaslightwala, A.; Szafranski, M. J.; Gaines, W. A. Removal of Oil and Grease and Chemical Oxygen Demand from Oily Automotive Wastewater by Adsorption after Chemical De-Emulsification. *Pract. Period. Hazard., Toxic, Radioact. Waste Manage.* **2003**, *7*, 156−162.

(6) Rawlins, C. H. Flotation of Fine Oil Droplets in Petroleum Production Circuits. In *Recent Advances in Mineral Processing Plant Design*; Elsevier, 2009.

(7) Saththasivam, J.; Loganathan, K.; Sarp, S. An Overview of Oil–Water Separation Using Gas Flotation Systems. *Chemosphere* **2016**, *144*, 671−680.

(8) Atarah, J. J. A. *The Use of Flotation Technology in Produced Water Treatment in the Oil & Gas Industry*; University of Stavanger: Norway, 2011.

(9) Al-Shamrani, A. A.; James, A.; Xiao, H. Separation of Oil from Water by Dissolved Air Flotation. *Colloids Surf., A* **2002**, *209*, 15−26.

(10) Feng, L.; Zhang, Z.; Mai, Z.; Ma, Y.; Liu, B.; Jiang, L.; Zhu, D. A Super-Hydrophobic and Super-Oleophilic Coating Mesh Film for the Separation of Oil and Water. *Angew. Chem., Int. Ed.* **2004**, *43*, 2012−2014.

(11) Wang, D.; McLaughlin, E.; Pfeffer, R.; Lin, Y. S. Adsorption of Oils from Pure Liquid and Oil–Water Emulsion on Hydrophobic Silica Aerogels. *Sep. Purif. Technol.* **2012**, *99*, 28−35.

(12) Janknecht, P.; Lopes, A. D.; Mendes, A. M. Removal of Industrial Cutting Oil from Oil Emulsions by Polymeric Ultra-and Microfiltration Membranes. *Environ. Sci. Technol.* **2004**, *38*, 4878−4883.

(13) Zhu, L.; Chen, M.; Dong, Y.; Tang, C. Y.; Huang, A.; Li, L. A Low-Cost Mullite-Titania Composite Ceramic Hollow Fiber Microfiltration Membrane for Highly Efficient Separation of Oil-in-Water Emulsion. *Water Res.* **2016**, *90*, 277−285.

(14) Nazzal, F. F.; Wiesner, M. R. Microfiltration of Oil-in-Water Emulsions. *Water Environ. Res.* **1996**, *68*, 1187−1191.

(15) Pope, J. M.; Yao, S.; Fane, A. G. Quantitative Measurements of the Concentration Polarisation Layer Thickness in Membrane Filtration of Oil-Water Emulsions Using NMR Micro-Imaging. *J. Membr. Sci.* **1996**, *118*, 247−257.

(16) Holdich, R. G.; Cumming, I. W.; Smith, I. D. Crossflow Microfiltration of Oil in Water Dispersions Using Surface Filtration with Imposed Fluid Rotation. *J. Membr. Sci.* **1998**, *143*, 263−274.

(17) Cumming, I. W.; Holdich, R. G.; Smith, I. D. The Rejection of Oil by Microfiltration of a Stabilised Kerosene/Water Emulsion. *J. Membr. Sci.* **2000**, *169*, 147−155.

(18) Ullah, A.; Starov, V. M.; Naeem, M.; Holdich, R. G. Microfiltration of Deforming Oil Droplets on a Slotted Pore Membrane and Sustainable Flux Rates. *J. Membr. Sci.* **2011**, *382*, 271−277.

(19) Ullah, A.; Habib, M.; Khan, S. W.; Ahmad, M. I.; Starov, V. M. Membrane Oscillation and Oil Drop Rejection during Produced Water Purification. *Sep. Purif. Technol.* **2015**, *144*, 16−22.

(20) Ullah, A.; Holdich, R. G.; Naeem, M.; Starov, V. M. Stability and Deformation of Oil Droplets during Microfiltration on a Slotted Pore Membrane. *J. Membr. Sci.* **2012**, *401−402*, 118−124.

(21) Lee, S.; Aurelle, Y.; Roques, H. Concentration Polarization, Membrane Fouling and Cleaning in Ultrafiltration of Soluble Oil. *J. Membr. Sci.* **1984**, *19*, 23−38.

(22) Lipp, P.; Lee, C. H.; Fane, A. G.; Fell, C. J. D. A Fundamental Study of the Ultrafiltration of Oil-Water Emulsions. *J. Membr. Sci.* **1988**, *36*, 161−177.

(23) Nabi, N.; Aimar, P.; Meireles, M. Ultrafiltration of an Olive Oil Emulsion Stabilized by an Anionic Surfactant. *J. Membr. Sci.* **2000**, *166*, 177−188.

(24) Chakrabarty, B.; Ghoshal, A. K.; Purkait, M. K. Ultrafiltration of Stable Oil-in-Water Emulsion by Polysulfone Membrane. *J. Membr. Sci.* **2008**, *325*, 427−437.

(25) Falahati, H.; Tremblay, A. Y. Flux Dependent Oil Permeation in the Ultrafiltration of Highly Concentrated and Unstable Oil-in-Water Emulsions. *J. Membr. Sci.* **2011**, *371*, 239−247.

(26) Lu, D.; Zhang, T.; Ma, J. Ceramic Membrane Fouling during Ultrafiltration of Oil/Water Emulsions: Roles Played by Stabilization Surfactants of Oil Droplets. *Environ. Sci. Technol.* **2015**, *49*, 4235−4244.

(27) Mohammadi, T.; Kazemimoghadam, M.; Saadabadi, M. Modeling of Membrane Fouling and Flux Decline in Reverse Osmosis during Separation of Oil in Water Emulsions. *Desalination* **2003**, *157*, 369−375.

(28) Peng, H.; Volchek, K.; MacKinnon, M.; Wong, W. P.; Brown, C. E. Application on to Nanofiltration to Water Management Options for Oil Sands Operation. *Desalination* **2004**, *170*, 137−150.

(29) Ullah, A.; Khan, S. W.; Shakoor, A.; Starov, V. M. Passage and Deformation of Oil Drops through Non-Converging and Converging Micro-Sized Slotted Pore Membranes. *Sep. Purif. Technol.* **2013**, *119*, 7−13.

(30) Tanaka, T.; Nishimoto, T.; Tsukamoto, K.; Yoshida, M.; Kouya, T.; Taniguchi, M.; Lloyd, D. R. Formation of Depth Filter Microfiltration Membranes of Poly (l-Lactic Acid) via Phase Separation. *J. Membr. Sci.* **2012**, *396*, 101−109.

(31) Frey, J. M.; Schmitz, P. Particle Transport and Capture at the Membrane Surface in Cross-Flow Microfiltration. *Chem. Eng. Sci.* **2000**, *55*, 4053−4065.

(32) Chandler, M.; Zydney, A. Effects of Membrane Pore Geometry on Fouling Behavior during Yeast Cell Microfiltration. *J. Membr. Sci.* **2006**, *285*, 334−342.

(33) Kuiper, S.; Brink, R.; Nijdam, W.; Krijnen, G. J. M.; Elwenspoek, M. C. Ceramic Microsieves: Influence of Perforation Shape and Distribution on Flow Resistance and Membrane Strength. *J. Membr. Sci.* **2002**, *196*, 149−157.

(34) van Rijn, C. J. M.; Veldhuis, G. J.; Kuiper, S. Nanosieves with Microsystem Technology for Microfiltration Applications. *Nanotechnology* **1998**, *9*, 343−345.

(35) Kuiper, S.; van Rijn, C.; Nijdam, W.; Raspe, O.; van Wolferen, H.; Krijnen, G.; Elwenspoek, M. Filtration of Lager Beer with Microsieves: Flux, Permeate Haze and in-Line Microscope Observations. *J. Membr. Sci.* **2002**, *196*, 159−170.

(36) Ullah, A.; Naeem, M.; Holdich, R. G.; Starov, V. M.; Semenov, S. Microfiltration of Deforming Droplets. In *UK Colloids*; Springer, 2011; pp 107−110.

(37) Ullah, A.; Holdich, R. G.; Naeem, M.; Starov, V. M. Shear Enhanced Microfiltration and Rejection of Crude Oil Drops through a Slotted Pore Membrane Including Migration Velocities. *J. Memb. Sci.* **2012**, *421−422*, 69−74.

(38) Ullah, A.; Starov, V. M.; Naeem, M.; Holdich, R. G.; Semenov, S. Filtration of Suspensions Using Slit Pore Membranes. *Sep. Purif. Technol.* **2013**, *103*, 180−186.

(39) Ullah, A.; Holdich, R. G.; Naeem, M.; Khan, S. W.; Starov, V. M. Prediction of Size Distribution of Crude Oil Drops in the Permeate Using a Slotted Pore Membrane. *Chem. Eng. Res. Des.* **2014**, *92*, 2775−2781.

(40) Ullah, A.; Ahmad, J.; Khan, H.; Khan, S. W.; Zamani, F.; Hasan, S. W.; Starov, V. M.; Chew, J. W. Membrane Oscillation and Slot (Pore) Blocking in Oil−Water Separation. *Chem. Eng. Res. Des.* **2019**, *142*, 111−120.

(41) Kosvintsev, S. R.; Sutrisna, P. D.; Cumming, I. W.; Holdich, R. G.; Mason, G. The Passage of Deforming Drops through a Slotted Microfilter. *Chem. Eng. Res. Des.* **2007**, *85*, 530−536.

(42) Alanezi, Y. H. Crossflow Microfiltration of Oil from Synthetic Produced Water. Doctoral Dissertation, Loughborough University, 2009.

(43) Cumming, I. W.; Holdich, R. G.; Smith, I. D. The Rejection of Oil Using an Asymmetric Metal Microfilter to Separate an Oil in Water Dispersion. *Water Res.* **1999**, *33*, 3587−3594.